Platinum Chemistry

Two-Photon-Activated Ligand Exchange in Platinum(II) Complexes**

Yao Zhao, Gareth M. Roberts, Simon E. Greenough, Nicola J. Farrer, Martin J. Paterson, William H. Powell, Vasilios G. Stavros,* and Peter J. Sadler*

Two-photon absorption (TPA) was theoretically proposed in 1931;[1] (near-)simultaneous absorption of two photons (approximately 10^{-16} s) by an atom or molecule can drive a transition equivalent to the absorption of a single photon of twice the energy,[2] ultimately activating the same photophysical or photochemical processes induced by one-photon absorption (OPA).[2,3] However, TPA probabilities are typically extremely small, and the first experimental evidence of TPA was not obtained until the 1960s, using a ruby laser.[4] Now femtosecond (fs) laser systems, which generate very high instantaneous photon densities, have opened up a plethora of multiphoton applications,[5] such as fluorescence microscopy[6] and photodynamic therapy (PDT).[7]

Herein, we report the first TPA-induced ligand substitution on a square-planar Pt^{II} complex. We compare OPA with TPA, and we use linear and quadratic density functional response theory to identify the electronic transitions involved and rationalize the wavelength dependence of the TPA. There has been broad interest in controlling the reactivity of Pt^{II} centers because of the clinical use of Pt^{II} drugs for the treatment of cancer. Platinum anticancer prodrugs such as Pt^{IV} diazidodihydroxido complexes[8] and Pt^{IV} dichloridodihydroxido or tetrachlorido complexes[9] are effective with OPA using UVA, or blue light, and are thus more suitable for surface tumors, whereas deeper tissue penetration requires longer wavelengths (620–850 nm).[10]

We designed the novel Pt^{II} complex, *cis*-[PtCl$_2$(MOPEP)$_2$] (**1**) containing the π-conjugated ligand 4-[2-(4-methoxyphenyl)ethynyl]pyridine (MOPEP) since we believed it would have potential for TPA. Reported work has shown that large TPA cross-sections (δ) are often associated with long, coplanar π-conjugated chains with opposing terminal donor and acceptor (D-A) moieties.[2,11] Complex **1** was synthesized as shown in Scheme 1. The *cis* geometry of the product was determined by ^{195}Pt NMR spectroscopy (see Supporting Information).
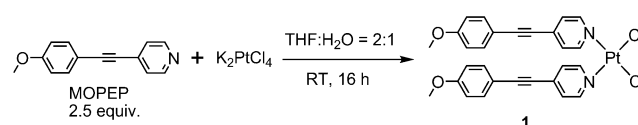
Scheme 1. Synthesis of the complex *cis*-[PtCl$_2$(MOPEP)$_2$] (**1**).

The absorption spectra of **1** and MOPEP in acetonitrile (MeCN) are shown in the Supporting Information, Figure S3. MOPEP has two major absorption bands centered at $\lambda = 297$ nm and 310 nm, which are both assigned to intramolecular charge-transfer (CT) transitions. The absorption centered at 344 nm for **1** can be assigned to a number of metal-to-ligand charge-transfer (MLCT) transitions; see Supporting Information for further details. In MeCN, **1** has no absorbance greater than 500 nm and is stable in the dark and upon irradiation with light $\lambda > 500$ nm. **1** was also stable in MeCN when heated to 343–353 K (MeCN b.p. = 355 K). The melting of **1** was investigated and decomposition was observed only above 473 K.

The photodecomposition of **1** in MeCN following OPA was studied by UV/Vis absorption spectroscopy. Upon irradiation of **1** with UVA ($\lambda = 330$–380 nm, Figure 1a) or broadband white light ($\lambda = 400$–700 nm, Figure 1b), the intensity of the major absorption band for **1** (at 344 nm) decreased. After irradiation with UVA for five minutes (Figure 1a, green curve) or white light for 30 minutes (Figure 1b, magenta curve), the absorbance at 344 nm disappeared, indicating complete photodecomposition of **1**. Concomitantly, two strong absorption bands at approximately 300 nm emerged in the spectra; these display the same spectral profile as the MOPEP ligand (Figure S3). This suggests that photodecomposition of **1** proceeds by substitution of the MOPEP ligands with solvent MeCN molecules (Scheme 2). After only one minute of irradiation with UVA, no recovery of **1** was observed (after 12 hours in the dark), as determined by UV/Vis spectroscopy. Notably, the rate of photodecomposition upon irradiation with UVA was much faster than with the broadband white light despite the lower power density of the UVA source. This is in agreement with

[*] Dr. Y. Zhao, Dr. G. M. Roberts,[+] S. E. Greenough,[+] Dr. N. J. Farrer, W. H. Powell, Prof. Dr. V. G. Stavros, Prof. Dr. P. J. Sadler
Department of Chemistry, University of Warwick
Coventry, CV4 7AL (UK)
E-mail: v.stavros@warwick.ac.uk
        p.j.sadler@warwick.ac.uk

Dr. M. J. Paterson
Institute of Chemical Sciences, Heriot-Watt University
Edinburgh, EH14 4AS (UK)

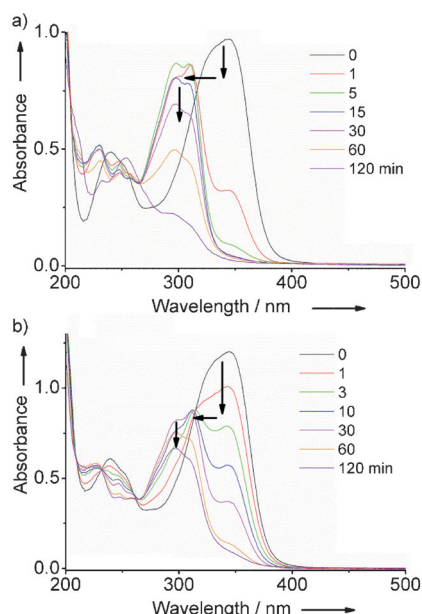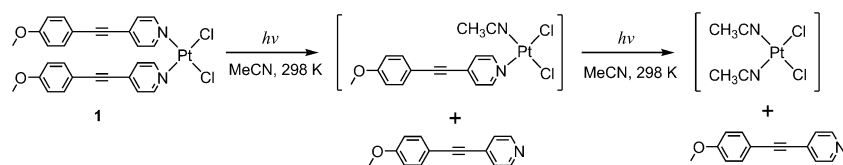[+] These authors contributed equally to this work.

Figure 1. Photoactivation of **1** upon irradiation with a) UVA and b) white light in MeCN at 298 K for various times followed by UV/Vis absorption spectroscopy.
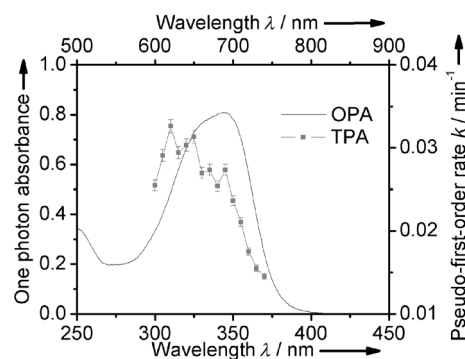

Figure 2. Wavelength dependence of pseudo-first-order rate constant (k) for TPA induced decomposition of **1** upon irradiation with femto-second laser pulses (■, top and right axes). For comparison, the UV/Vis spectrum of **1** is shown with a solid line (left and bottom axes).

Figure S3, which suggests that only light below approximately 430 nm in the white light continuum is effectively absorbed by **1**.

The photodecomposition of **1** in MeCN was also examined using 600 MHz ^{1}H NMR spectroscopy and HPLC-coupled MS analysis. The results of these analyses are consistent with the UV/Vis data (see Supporting Information). Irradiation over longer periods of time in both experiments (more than five minutes by UVA and more than 30 minutes by white light) caused the major absorption bands corresponding to free MOPEP to decay in intensity, suggesting additional decomposition of the photodissociated MOPEP ligand (see Supporting Information).

When a solution of **1** in MeCN was irradiated with focused femtosecond laser pulses, at wavelengths of 600–740 nm, a decrease in the intensity of the major absorption band for **1** ($\lambda = 344$ nm) was observed, analogous to the OPA measurements. The reaction mixture was analyzed by ESI-MS and a signal for the MOPEP ligand ($m/z = 210.1$ for $[M+H]^+$) was observed. HPLC was also used to analyze the photoproducts from TPA activation. Figures S6 f, g are the chromatograms of **1** in MeCN upon irradiation with a femtosecond laser at 640 nm for 15 and 45 minutes, respectively. They show that free MOPEP ligands and a small amount of [PtCl₂(MOPEP)-(MeCN)] are produced after 15 minutes of TPA activation, and that **1** was completely photodegraded after 45 minutes.

These measurements suggest that the reaction initiated by TPA follows the same course as that from OPA using UVA light.

The wavelength dependence of TPA-induced decomposition between 600 and 740 nm, was monitored by UV/Vis spectroscopy. This TPA wavelength range correlates with the maximum OPA absorption band for **1** in Figure 2. The photon density per femtosecond laser pulse (photons cm^{-2} pulse^{-1}) was maintained constant across the entire wavelength range (see Supporting Information). The pseudo-first-order photodecomposition rate constants (k) were calculated from the decrease in absorbance at 344 nm at each TPA wavelength and are plotted in Figure 2.

Several control experiments were also carried out. Irradiation with an unfocused femtosecond laser at 700 nm resulted in negligible TPA-induced decomposition of **1**, whereas OPA from an unfocused femtosecond laser between 300–400 nm did activate photodecomposition. These control experiments confirm that when the photon density of red light (600–740 nm) is sufficiently high, TPA induced decomposition of **1** can be readily initiated.

Figure 2 highlights that the wavelength for the maximum observed value for k (approximately 620 nm) appears blue-shifted (by about 70 nm) with respect to the corresponding maximum for the OPA peak ($2\lambda \approx 690$ nm). To further understand this shift, linear and quadratic density functional response theory calculations were carried out to determine both the OPA oscillator strengths and TPA cross-sections for the electronic transitions of **1** (Figure 3 a, Table S3), using the CAM-B3LYP functional.[12] OPA calculations were performed using standard linear-response time-dependent density functional theory (TD-DFT) as implemented in Gaussian 09,[13] while the TPA cross-sections were obtained as the single residue of the quadratic response function in the Dalton 2.0 program.[14] It is only recently that accurate TPA data have been obtained from computation owing to advances in non-linear response theory.[2, 15] Specifically, the response theory approach obviates the need for the explicit construction of sum-over-states expressions. Thus, the chosen functional needs to be more robust than for
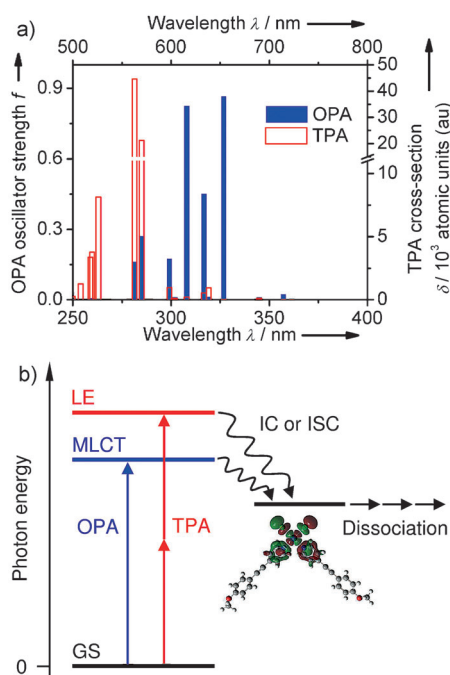

Scheme 2. Photoinduced decomposition pathways for **1**.

Figure 3. a) Density functional response theory calculated OPA oscillator strengths, f (blue, left and bottom axes) and TPA cross-sections, δ (red, top and right axes) for **1** in the gas phase (for further details see Supporting Information). b) Schematic diagram of the dissociation mechanism following OPA and TPA. GS = ground state; LE = localized CT state on MOPEP ligands.

standard TD-DFT, and CAM-B3LYP proves to be an optimal choice.[16] TPA tensor components were combined to give rotationally averaged TPA cross-sections (see Supporting Information for further calculation details). The results of the OPA calculations (Figure 3a, blue bars) are in reasonable accord with the experimental UV/Vis spectrum (Figure 2), displaying the largest oscillator strengths between 308–327 nm. It is notable that OPA calculations determine the maximum OPA absorbance to be approximately 30 nm shorter than the experimentally observed maximum, most likely because of effects of the MeCN solvent which are not captured in our calculations on the isolated "gas phase" species.[17] The calculations characterize these strong OPA transitions as MLCT states (see Supporting Information). Additionally, the DFT response calculations also determine four very weak transitions between 345–361 nm, which possess dissociative character with respect to all M−L bonds (see inset molecular orbital in Figure 3b). This leads us to postulate that after initial OPA to the stronger MLCT transitions, rapid internal conversion (IC) to these lower energy dissociative states occurs (or intersystem crossing (ISC) to the equivalent triplet states), causing cleavage of the Pt−MOPEP bonds; such a mechanism is schematically summarized in Figure 3b. Further elucidation of this photophysical mechanism ultimately requires high-level multiconfigurational ab initio calculations,[18] beyond the scope of the present work. Most reassuringly though, Figure 3a shows that the calculated TPA maxima at 570 nm and 562 nm (corresponding to CT transitions localized on the MOPEP

ligands; see Supporting Information) lie at TPA wavelengths around 70 nm shorter than the calculated OPA maximum, in excellent agreement with our experimental observations. In contrast, however, the MLCT states (which exhibit the largest OPA oscillator strengths) possess only minor TPA cross-sections. This also corresponds with the experimentally observed blue-shift for the TPA maximum relative to the OPA maximum, and further explains why the traditional expectation that $\lambda_{TPA} \approx 2\lambda_{OPA}$[3,19] is not observed for **1**.

In conclusion, we report the first TPA-induced ligand substitution for a square-planar complex; the dissociation of the pyridine derivative MOPEP from *cis*-[PtCl$_2$(MOPEP)$_2$]. The MOPEP ligands exhibit very efficient photolability upon irradiation with UVA, visible, and also femtosecond laser irradiation between 600 nm and 740 nm. The enhanced photolabilization demonstrated here may be useful in the design of novel photoactivatable platinum chemotherapeutic agents in situations where deep tissue penetration is needed.

[1] M. Göppert-Mayer, *Ann. Phys.* **1931**, *401*, 273–294.
[2] M. Pawlicki, H. A. Collins, R. G. Denning, H. L. Anderson, *Angew. Chem.* **2009**, *121*, 3292–3316; *Angew. Chem. Int. Ed.* **2009**, *48*, 3244–3266.
[3] J. E. Rogers, J. E. Slagle, D. M. Krein, A. R. Burke, B. C. Hall, A. Fratini, D. G. McLean, P. A. Fleitz, T. M. Cooper, M. Drobizhev, N. S. Makarov, A. Rebane, K. Y. Kim, R. Farley, K. S. Schanze, *Inorg. Chem.* **2007**, *46*, 6483–6494.
[4] W. Kaiser, C. G. B. Garrett, *Phys. Rev. Lett.* **1961**, *7*, 229–231.
[5] a) M. Salierno, E. Marceca, D. S. Peterka, R. Yuste, R. Etchenique, *J. Inorg. Biochem.* **2010**, *104*, 418–422; b) M. Four, D. Riehl, O. Mongin, M. Blanchard-Desce, L. M. Lawson-Daku, J. Moreau, J. Chauvin, J. A. Delaire, G. Lemercier, *Phys. Chem. Chem. Phys.* **2011**, *13*, 17304–17312.
[6] S. W. Botchway, M. Charnley, J. W. Haycock, A. W. Parker, D. L. Rochester, J. A. Weinstein, J. A. G. Williams, *Proc. Natl. Acad. Sci. USA* **2008**, *105*, 16071–16076.
[7] a) V. Nikolenko, R. Yuste, L. Zayat, L. M. Baraldo, R. Etchenique, *Chem. Commun.* **2005**, 1752–1754; b) H. A. Collins, M. Khurana, E. H. Moriyama, A. Mariampillai, E. Dahlstedt, M. Balaz, M. K. Kuimova, M. Drobizhev, V. X. D. Yang, D. Phillips, A. Rebane, B. C. Wilson, H. L. Anderson, *Nat. Photonics* **2008**, *2*, 420–424.
[8] N. J. Farrer, J. A. Woods, L. Salassa, Y. Zhao, K. S. Robinson, G. Clarkson, F. S. Mackay, P. J. Sadler, *Angew. Chem.* **2010**, *122*, 9089–9092; *Angew. Chem. Int. Ed.* **2010**, *49*, 8905–8908.
[9] a) L. Cubo, A. M. Pizarro, A. G. Quiroga, L. Salassa, C. Navarro-Ranninger, P. J. Sadler, *J. Inorg. Biochem.* **2010**, *104*, 909–918; b) C. Loup, A. Tesouro Vallina, Y. Coppel, U. Létinois, Y. Nakabayashi, B. Meunier, B. Lippert, G. Pratviel, *Chem. Eur. J.* **2010**, *16*, 11420–11431.
[10] a) K. Ogawa, Y. Kobuke, *Anti-Cancer Agents Med. Chem.* **2008**, *8*, 269–279; b) L. Carroll, T. R. Humphreys, *Clin. Dermatol.* **2006**, *24*, 2–7.
[11] G. S. He, L.-S. Tan, Q. Zheng, P. N. Prasad, *Chem. Rev.* **2008**, *108*, 1245–1330.
[12] T. Yanai, D. P. Tew, N. C. Handy, *Chem. Phys. Lett.* **2004**, *393*, 51–57.

[13] M. J. Frisch, et al., Gaussian 09, Revision A.02; Gaussian, Inc., Wallingford CT, **2009**.

[14] Dalton, a molecular electronic structure program, Release 2.0, **2005**, see http://www.kjemi.uio.no/software/dalton/dalton.html.

[15] a) J. Arnbjerg, M. J. Paterson, C. B. Nielsen, M. Jørgensen, O. Christiansen, P. R. Ogilby, *J. Phys. Chem. A* **2007**, *111*, 5756–5767; b) M. Johnsen, M. J. Paterson, J. Arnbjerg, O. Christiansen, C. B. Nielsen, M. Jorgensen, P. R. Ogilby, *Phys. Chem. Chem. Phys.* **2008**, *10*, 1177–1191; c) J. Arnbjerg, A. Jiménez-Banzo, M. J. Paterson, S. Nonell, J. I. Borrell, O. Christiansen, P. R. Ogilby, *J. Am. Chem. Soc.* **2007**, *129*, 5188–5199.

[16] M. J. Paterson, O. Christiansen, F. Pawlowski, P. Jorgensen, C. Hattig, T. Helgaker, P. Salek, *J. Chem. Phys.* **2006**, *124*, 054322.

[17] R. S. Butler, P. Cohn, P. Tenzel, K. A. Abboud, R. K. Castellano, *J. Am. Chem. Soc.* **2009**, *131*, 623–633.

[18] J. M. Żurek, M. J. Paterson, *J. Phys. Chem. A* **2012**, *116*, 5375–5382.

[19] A. Picot, F. Malvolti, B. Le Guennic, P. L. Baldeck, J. A. G. Williams, C. Andraud, O. Maury, *Inorg. Chem.* **2007**, *46*, 2659–2665.